Discretizing Wachspress kernels is safe

Kai Hormann · Jiří Kosinka

Abstract

Barycentric coordinates were introduced by Möbius in 1827 as an alternative to Cartesian coordinates. They describe points relative to the vertices of a simplex and are commonly used to express the linear interpolant of data given at these vertices. Generalized barycentric coordinates and kernels extend this idea from simplices to polyhedra and smooth domains. In this paper, we focus on Wachspress coordinates and Wachspress kernels with respect to strictly convex planar domains. Since Wachspress kernels can be evaluated analytically only in special cases, a common way to approximate them is to discretize the domain by an inscribed polygon and to use Wachspress coordinates, which have a simple closed form. We show that this discretization, which is known to converge quadratically, is safe in the sense that the Wachspress coordinates used in this process are well-defined not only over the inscribed polygon, but over the entire original domain.

Citation Info

Journal
Computer Aided Geometric Design

Volume
52–53, March–April 2017

Pages
126–134

Note
Proceedings of GMP

1 Introduction

Let $\Psi \subset \mathbb{R}^2$ be a bounded, open, and strictly convex planar domain with boundary $\partial\Psi$ given by a C^2 continuous parametric curve $p\colon [a,b] \to \mathbb{R}^2$, injective on $[a,b)$ with $p(a) = p(b)$. By strict convexity we mean that $\partial\Psi$ does not contain straight segments, so that for any $t \in [a,b]$ the intersection of the tangent of p at $p(t)$ with $\bar{\Psi}$ is just $\{p(t)\}$. The *Wachspress kernel* $b\colon \bar{\Psi} \times [a,b] \to \mathbb{R}$ for Ψ is then defined as [10]

$$b(v,t) = \frac{w(v,t)}{\int_a^b w(v,s)\,\mathrm{d}s} \qquad \text{with} \qquad w(v,t) = \frac{p'(t) \times p''(t)}{\big((p(t)-v) \times p'(t)\big)^2}. \tag{1}$$

This kernel is *non-negative*,

$$b(v,t) \geqslant 0, \qquad v \in \bar{\Psi}, \quad t \in [a,b],$$

satisfies the *partition of unity* property

$$\int_a^b b(v,t)\,\mathrm{d}t = 1, \qquad v \in \bar{\Psi},$$

and the *linear precision* property

$$\int_a^b b(v,t)p(t)\,\mathrm{d}t = v, \qquad v \in \bar{\Psi}.$$

It can be understood as the transfinite counterpart of Wachspress coordinates [8], a special case of generalized barycentric coordinates [1]. The main application of Wachspress kernels is transfinite interpolation [3]. Given a continuous function $f\colon [a,b] \to \mathbb{R}^d$, the *transfinite Wachspress interpolant* $g\colon \bar{\Psi} \to \mathbb{R}^d$ of the boundary data $f \circ p^{-1}\colon \partial\Psi \to \mathbb{R}^d$ is defined as

$$g(v) = \int_a^b b(v,t)f(t)\,\mathrm{d}t. \tag{2}$$

For example, if $d = 1$, then this interpolant can be used to interpolate boundary values, like height values [10], for $d = 2$, it gives rise to injective mappings between convex domains [2], which in turn can be used for planar free-form shape deformation [10], and potential applications in the case $d = 3$ include colour interpolation [10] and surface patch design. Despite their analytic form, the kernel and the interpolant need to be handled numerically in practical applications. One option is to *approximate* the integrals in (1) and (2) with Gaussian Quadrature or Newton–Cotes formulas [7]. Another option is to *discretize* the domain by an inscribed polygon and to consider Wachspress coordinates for that polygon [5].

We follow the latter approach. In this setting, the inscribed polygon P is a strictly convex polygon, viewed as an open set, with n vertices $v_i = p(t_i)$, $i = 1,\dots,n$ on $\partial\Psi$ for certain parameter values $a \leqslant t_1 < t_2 < \cdots <$

$t_n < b$. We consider indices cyclic over the range $1,\dots,n$, so that $v_0 = v_n$ and $v_{n+1} = v_1$, and denote the signed areas of the triangles $[v, v_i, v_{i+1}]$ and $[v_{i-1}, v_i, v_{i+1}]$ by $A_i(v)$ and C_i, respectively; see Figure 1, left. Note that strict convexity ensures that no three vertices of P are collinear, hence $C_i > 0$. The *Wachspress coordinates* $b_i \colon \bar{P} \to \mathbb{R}$, $i = 1,\dots,n$ for P are then defined as [8, 6]

$$b_i(v) = \frac{w_i(v)}{W(v)}, \tag{3}$$

where the numerator

$$w_i(v) = C_i \prod_{\substack{j=1 \\ j \neq i-1,i}}^{n} A_j(v)$$

is a polynomial of degree at most $n-2$ and the denominator

$$W(v) = \sum_{i=1}^{n} w_i(v)$$

is a polynomial of degree at most $n-3$, also known as the *adjoint polynomial* of P. The coordinates b_i are well-defined and non-negative over $\bar{P}$, and they satisfy the discrete counterparts of the partition of unity and linear precision property above, as well as the *Lagrange property* $b_i(v_j) = \delta_{i,j}$, $i, j = 1,\dots,n$. The interpolant in (2) can then be approximated by the *discrete Wachspress interpolant* $g_h \colon \bar{P} \to \mathbb{R}^d$, which is defined as

$$g_h(v) = \sum_{i=1}^{n} b_i(v) f(v_i), \tag{4}$$

where $h = \max_{i=1,\dots,n}(t_{i+1} - t_i)$ with $t_{n+1} = t_1 + b - a$ is the maximum parametric distance between neighbouring vertices of P. It was shown in [5] that g_h converges quadratically to g as $h \to 0$.

A potential problem with this approach is that Wachspress coordinates have unremovable singularities along the *adjoint curve*

$$\Gamma = \{v \in \mathbb{R}^2 : W(v) = 0\}.$$

Hence, it seems natural to ask the question, "Are Γ and $\bar{\Psi}$ disjoint?" Or, put differently, "Are the coordinates b_i and the interpolant g_h well-defined over $\bar{\Psi}$?" Based on their numerical results, Kosinka and Bartoň [5] conjecture a positive answer, and the goal of this paper is to prove that their conjecture is correct (Section 2). The main implication of this result is that Wachspress coordinates and interpolants for a polygon P inscribed in Ψ can be safely used over $\bar{\Psi}$ and do not have to be trimmed to $\bar{P}$ (Section 3). In particular, this allows us to study the convergence rate for points on $\partial\Psi$, and our numerical results suggest that this rate is actually cubic (Section 4).

2 Wachspress coordinates outside the defining polygon

Let $L_i = \{(1-\lambda)v_i + \lambda v_{i+1} : \lambda \in \mathbb{R}\}$ be the line through v_i and v_{i+1} for $i = 1,\dots,n$, and denote the intersection of L_i and L_j by $\hat{v}_{i,j}$ for $i \neq j$; see Figure 1, right. If L_i and L_j are parallel, then $\hat{v}_{i,j}$ is at infinity, in the direction of L_i and L_j. Moreover, $\hat{v}_{i,i-1} = v_i$ and $\hat{v}_{i,i+1} = v_{i+1}$, and all other $\hat{v}_{i,j}$ with $j \neq i-1, i, i+1$ are called the *exterior intersection points* of P. We denote the set of all exterior intersection points by

$$\hat{V} = \{\hat{v}_{i,j} : i, j = 1,\dots,n \wedge j \neq i-1, i, i+1\}.$$

Note that $|\hat{V}| = n(n-3)/2$ and that the adjoint polynomial W is the unique polynomial (up to multiplication by a constant) of degree at most $n-3$ that vanishes at all $\hat{v} \in \hat{V}$ [8, 9]. We start by studying the behaviour of Wachspress coordinates along the lines L_i.

Proposition 1. *Wachspress coordinates are well-defined and linear over $L_i \setminus \hat{V}$ for $i = 1,\dots,n$.*

Proof. For $v = (1-\lambda)v_i + \lambda v_{i+1} \in L_i$ we have $A_i(v) = 0$, so that $w_j(v) = 0$ for $j \neq i, i+1$, as well as $A_{i-1}(v) = \lambda A_{i-1}(v_{i+1}) = \lambda C_i$ and $A_{i+1}(v) = (1-\lambda)A_{i+1}(v_i) = (1-\lambda)C_{i+1}$. Consequently,

$$W(v) = w_i(v) + w_{i+1}(v) = \big(C_i A_{i+1}(v) + C_{i+1} A_{i-1}(v)\big) \prod_{\substack{j=1 \\ j \neq i-1,i,i+1}}^{n} A_j(v) = C_i C_{i+1} \prod_{\substack{j=1 \\ j \neq i-1,i,i+1}}^{n} A_j(v)$$

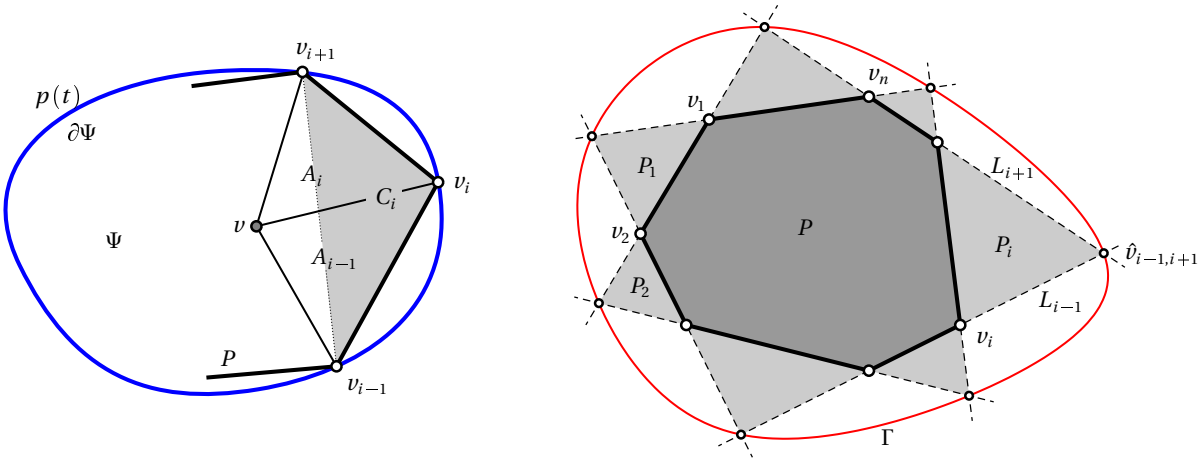

Figure 1: Left: Notation used in the definition of Wachspress coordinates and the Wachspress kernel, where C_i is the area of the shaded triangle. Right: Notation used to prove our main result.

and $W(v) \neq 0$ for $v \in L_i \backslash \hat{V}$, because this restriction of v guarantees that the areas $A_j(v)$ in the product do not vanish. By (3), we then have

$$b_i(v) = \frac{A_{i+1}(v)}{C_{i+1}} = 1 - \lambda, \qquad b_{i+1}(v) = \frac{A_{i-1}(v)}{C_i} = \lambda,$$

and $b_j(v) = 0$ for $j \neq i, i+1$. □

Now that we have clarified the behaviour along the lines L_i, we focus on the open regions

$$P_i = \{ v \in \mathbb{R}^2 : A_{i-1}(v) > 0 \wedge A_i(v) < 0 \wedge A_{i+1} > 0 \}, \qquad i = 1, \ldots, n,$$

as shown in Figure 1, right. Note that P_i extends to infinity if L_{i-1} and L_{i+1} are parallel or happen to intersect on the left of L_i, that is, if $A_i(\hat{v}_{i-1,i+1}) > 0$. Our main goal is to show that Wachspress coordinates are well-defined over

$$\hat{P} = \bigcup_{i=1}^{n} P_i,$$

but we first need a preliminary result.

To this end, let $L = \bigcup_{i=1}^{n} L_i$ be the union of all lines defined by the edges of P and consider $v \in \mathbb{R}^2 \backslash L$. For any such v, we have $A_i(v) \neq 0$ for $i = 1, \ldots, n$, so that the scaled Wachspress weights

$$\tilde{w}_i(v) = \frac{w_i(v)}{\prod_{j=1}^{n} A_j(v)} = \frac{C_i}{A_{i-1}(v) A_i(v)}$$

and their sum

$$\tilde{W}(v) = \sum_{i=1}^{n} \tilde{w}_i(v)$$

are well-defined. We further call a convex polygon P' a *refinement* of P if P' has $n+1$ vertices $v'_1, \ldots, v'_{n+1}$, where $v'_i = v_i$ for $i = 1, \ldots, n$; see Figure 2. Other notation with a prime, such as A'_i and W', is also understood with respect to P'. In this setting we can state precisely how the denominator $\tilde{W}$ reacts to such a refinement.

Lemma 2. *If P' is a refinement of P and $v \in \mathbb{R}^2 \backslash (L \cup L')$, then*

$$\tilde{W}'(v) = \tilde{W}(v) - \frac{C'_{n+1}}{A_n(v)} \tilde{w}'_{n+1}(v). \tag{5}$$

Proof. We first assume that v is not on the line parallel to L_n through v'_{n+1}, so that L_n and the line through v and v'_{n+1} cross at some point u that can be expressed as

$$u = (1-\lambda) v_n + \lambda v_1 = (1-\mu) v + \mu v'_{n+1} \tag{6}$$

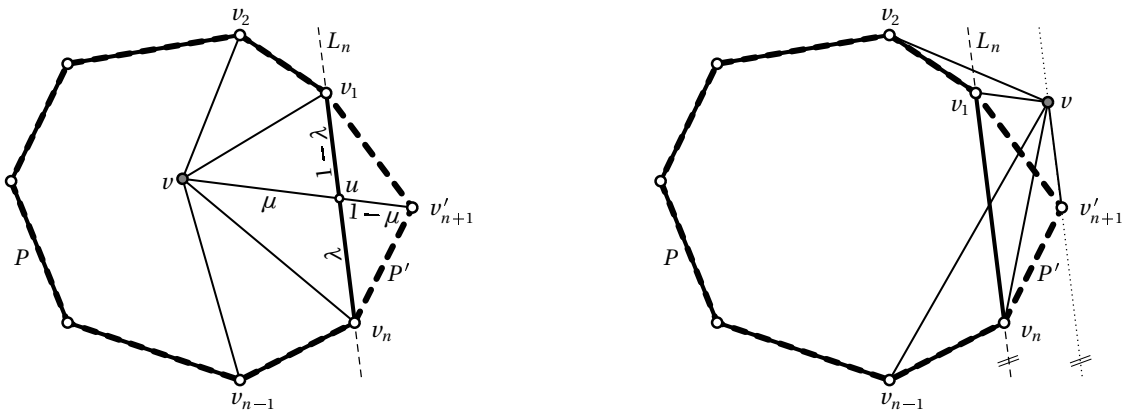

Figure 2: Notation used in the proof of Lemma 2. The polygon P is marked by thick solid lines, and its refinement P' by thick dashed lines.

for some $\lambda, \mu \in \mathbb{R}$ and $\mu \neq 0$; see Figure 2, left. Since $A'_i(v) = A_i(v)$ for $i = 1, \ldots, n-1$ and $C'_i = C_i$ for $i = 2, \ldots, n-1$, we have $\tilde{w}'_i(v) = \tilde{w}_i(v)$ for $i = 2, \ldots, n-1$, and it remains to focus on the three scaled weights $\tilde{w}'_i(v)$ for $i = n, n+1, 1$. It follows from (6) that

$$A_{n-1}(u) = \lambda C_n = (1-\mu)A_{n-1}(v) + \mu C'_n$$

and

$$\mu A'_n(v) = \mathrm{Area}[v_n, u, v] = \lambda A_n(v),$$

hence

$$\tilde{w}'_n(v) = \frac{C'_n}{A'_{n-1}(v)A'_n(v)} = \frac{\lambda C_n - (1-\mu)A_{n-1}(v)}{\mu A_{n-1}(v)A'_n(v)} = \tilde{w}_n(v) - \frac{1-\mu}{\mu}\frac{1}{A'_n(v)},$$

and similarly

$$\tilde{w}'_1(v) = \tilde{w}_1(v) - \frac{1-\mu}{\mu}\frac{1}{A'_{n+1}(v)}.$$

Moreover, we observe that

$$\frac{C'_{n+1}}{A_n(v)} = \frac{1-\mu}{\mu}$$

and

$$C'_{n+1} + A_n(v) = A'_n(v) + A'_{n+1}(v),$$

and the statement then follows, because

$$\begin{aligned}
\tilde{w}'_n(v) + \tilde{w}'_{n+1}(v) + \tilde{w}'_1(v) &= \tilde{w}_n(v) + \tilde{w}_1(v) - \frac{C'_{n+1}}{A_n(v)}\left(\frac{1}{A'_n(v)} - \frac{A_n(v)}{C'_{n+1}}\tilde{w}'_{n+1}(v) + \frac{1}{A'_{n+1}(v)}\right) \\
&= \tilde{w}_n(v) + \tilde{w}_1(v) - \frac{C'_{n+1}}{A_n(v)}\left(\frac{A'_{n+1}(v) - A_n(v) + A'_n(v)}{A'_n(v)A'_{n+1}(v)}\right) \\
&= \tilde{w}_n(v) + \tilde{w}_1(v) - \frac{C'_{n+1}}{A_n(v)}\tilde{w}'_{n+1}(v).
\end{aligned}$$

If v lies on the line parallel to L_n through v'_{n+1} (see Figure 2, right), then

$$v = v'_{n+1} + \lambda(v_1 - v_n)$$

for some $\lambda \in \mathbb{R}$, hence

$$A_{n-1}(v) = C'_n + \lambda C_n$$

and

$$A'_n(v) = \lambda C'_{n+1} = -\lambda A_n(v),$$

so that

$$\tilde{w}'_n(v) = \frac{-\lambda C_n + A_{n-1}(v)}{A_{n-1}(v)A'_n(v)} = \tilde{w}_n(v) + \frac{1}{A'_n(v)}.$$

Likewise, we get

$$\tilde{w}'_1(v) = \tilde{w}_1(v) + \frac{1}{A'_{n+1}(v)},$$

and the statement follows, because $A'_{n+1}(v) = -A'_n(v)$ and $C'_{n+1}/A_n(v) = -1$. □

It is interesting to note that $-C'_{n+1}/A_n(v)$ is the barycentric coordinate of v'_{n+1} corresponding to v with respect to the triangle $[v, v_n, v_1]$ and that (5) also holds for mean value coordinates [4]. With the help of Lemma 2, we can now prove our main result.

Theorem 3. *Wachspress coordinates are well-defined over $\hat{P}$.*

Proof. Without loss of generality, we assume $v \in P_2$, so that $A_2(v) < 0$ and $A_i(v) > 0$ for $i \neq 2$. The key idea now is to first consider the quadrilateral $[v_1, v_2, v_3, v_4]$. For this quadrilateral it is clear that the coordinates are well-defined, because its adjoint curve Γ is the line through $\hat{v}_{1,3}$ and $\hat{v}_{2,4}$ and does not intersect P_2. More precisely, we have $W(v) > 0$, because P_2 is in the same half-plane with respect to Γ as P, and therefore $\tilde{W}(v) < 0$. We now refine the quadrilateral successively by inserting the vertices $v_5, \ldots, v_n$, one at a time. By Lemma 2, each refinement step subtracts a positive value from $\tilde{W}(v)$. For example, in the first step, when v_5 is added, we have

$$\tilde{W}'(v) = \tilde{W}(v) - \frac{C'_5}{A_4(v)}\tilde{w}'_5(v),$$

where C'_5, $A_4(v)$, and $\tilde{w}'_5(v)$ are all positive for $v \in P_2$. The "old" $\tilde{W}(v)$ is then updated to become the "new" $\tilde{W}'(v)$ without changing its sign. The subsequent steps proceed similarly for the other new vertices $v_6, \ldots, v_n$. Consequently, the inequality $\tilde{W}(v) < 0$ remains valid until we reach the original polygon with n vertices. □

Corollary 4. *Wachspress coordinates are well-defined over $\bar{\Psi}$.*

Proof. We first note that Wachspress coordinates are well-defined over $\bar{P}$, because P is strictly convex, and over $\hat{P}$ by Theorem 3, and so it remains to show that $\bar{\Psi} \subset \bar{P} \cup \hat{P}$. To this end, consider two consecutive vertices $v_i = p(t_i)$ and $v_{i+1} = p(t_{i+1})$ of P and the open arc $s_i = \{p(t) : t \in (t_i, t_{i+1})\}$ of $\partial\Psi$ between v_i and v_{i+1}. As P is inscribed in Ψ, the tangent of p at v_i lies in the sector between L_{i-1} and L_i, which also contains P_i and similarly for the tangent at v_{i+1}. The strict convexity of Ψ then implies that $s_i \subset P_i$ and further that $\bar{\Psi} \subset \bar{P} \cup \hat{P}$. □

Remark 5. It has not escaped our notice that the initial assumptions on the domain Ψ can be relaxed, and that our arguments extend, with minor modifications, to the setting where Ψ is a weakly convex domain with piecewise C^1 boundary, that is, p can have finitely many (convex) corners and may contain straight segments. We call a polygon P an *admissible discretization* of Ψ, if all vertices of P lie on $\partial\Psi$ and all straight segments of $\partial\Psi$ appear as edges of P. In particular, if Ψ is itself a polygon then $P = \Psi$ is the only admissible discretization. Note that the corners of $\partial\Psi$ do not necessarily have to be vertices of P. It follows from the convexity of Ψ that an admissible discretization P of Ψ is strictly convex, and so the Wachspress coordinates for P are well-defined over $\bar{P}$.

For such Ψ, the kernel $b(v,t)$ in (1) may not be well-defined and is instead understood as the limit of the convergent sequence of Wachspress coordinates defined over finer and finer admissible discretizations of Ψ [5]. While Theorem 3 still holds in this setting, the proof of Corollary 4 needs to be modified slightly. As above, we consider the open arc s_i of $\partial\Psi$, but now distinguish two cases. First, if s_i is a straight segment, then $s_i = [v_i, v_{i+1}]$, hence $s_i \subset \bar{P}$. Second, if s_i is not straight, then it follows from the convexity of Ψ and the fact that s_i does not contain straight sub-segments that $s_i \subset P_i$. Overall, this still shows that $\bar{\Psi} \subset \bar{P} \cup \hat{P}$.

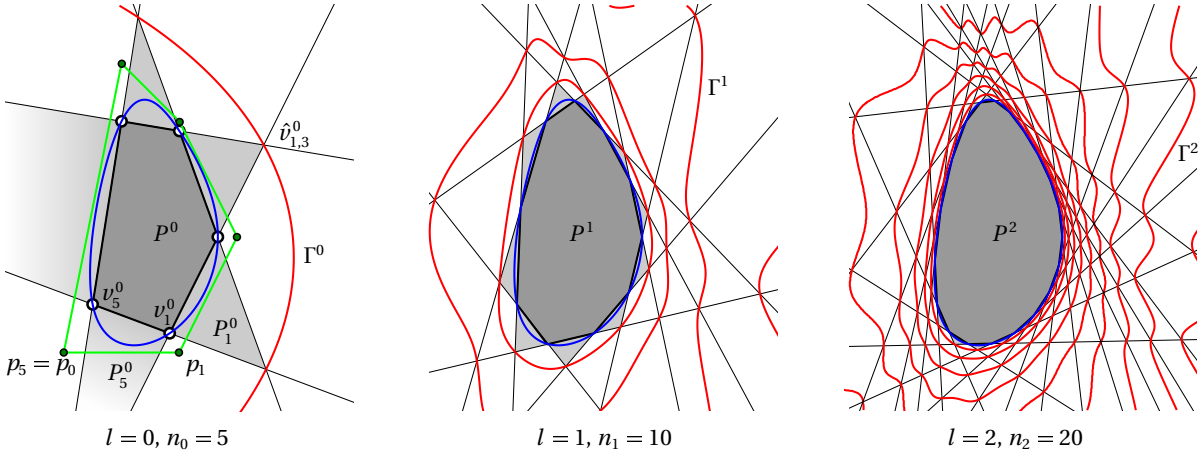

Figure 3: A sequence of polygons P^l (dark grey) inscribed in a smooth domain Ψ and the associated adjoint curves Γ^l (red) for $l = 0,1,2$. The boundary curve of Ψ (blue) is the periodic uniform cubic B-spline curve defined by the green control polygon. The adjoint curves touch $\hat{P}^l$ (light grey) at the exterior intersection points $\hat{v}^l_{i-1,i+1}$, but do not intersect $\hat{P}^l$.

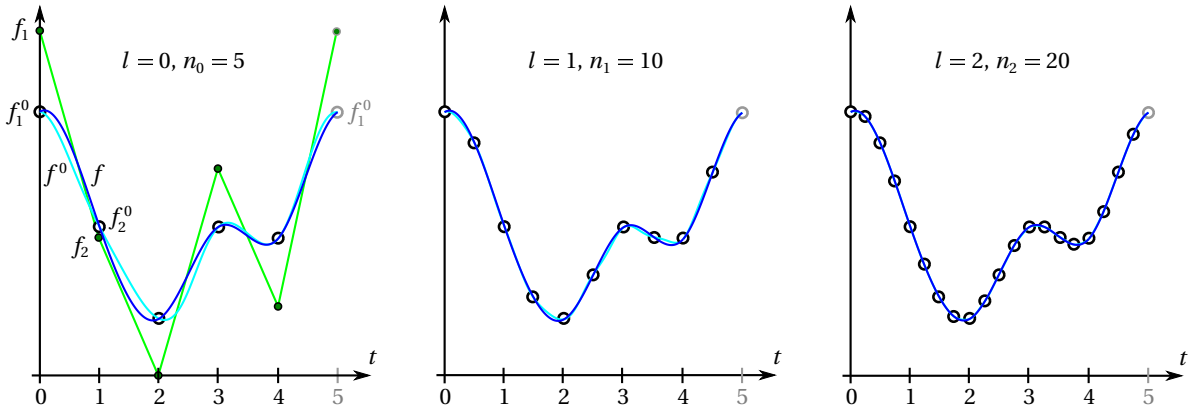

Figure 4: Approximation of the periodic uniform B-spline function f (blue) defined by the green control values over the boundary of Ψ (see Figure 3) by the restrictions f^l (cyan) of the discrete Wachspress interpolants to $\partial\Psi$ for $l = 0,1,2$.

3 Examples

Let us now illustrate the practical implications of Theorem 3 and Corollary 4. For the example in Figure 3, we took as boundary of Ψ a C^2 continuous periodic cubic B-spline curve

$$p\colon [0,5] \to \mathbb{R}^2, \qquad p(t) = \sum_{i=0}^{7} p_i N_i(t),$$

with control points $p_0,\dots,p_4,p_5 = p_0,p_6 = p_1,p_7 = p_2$ and cubic B-spline basis functions $N_0,\dots,N_7$ with respect to the uniform knot vector $(\tau_0,\tau_1,\dots,\tau_{11}) = (-3,-2,\dots,8)$. We further created a sequence of inscribed polygons P^l, $l \in \mathbb{N}_0$ with $n_l = 5\cdot 2^l$ vertices $v^l_i = p(t^l_i) \in \partial\Psi$ for uniformly spaced parameter values $t^l_i = (i-1)/2^l$, $i = 1,\dots,n_l$ and computed the adjoint curves Γ^l. Figure 3 shows how Γ^l becomes more and more complex as l increases, but does not intersect $\bar{P}^l \cup \hat{P}^l$, as predicted by Theorem 3.

It is further apparent from Figure 3 that $\bar{\Psi}$ is contained in $\bar{P}^l \cup \hat{P}^l$, as shown in the proof of Corollary 4, so that the transfinite Wachspress interpolant g in (2) can be approximated by the associated discrete Wachspress interpolants $g^l_{h_l}$ in (4) with $h_l = 1/2^l$ over $\bar{\Psi}$, and in particular over $\partial\Psi$. For the example in Figure 4, we took the same domain as in Figure 3 and considered the transfinite Wachspress interpolant

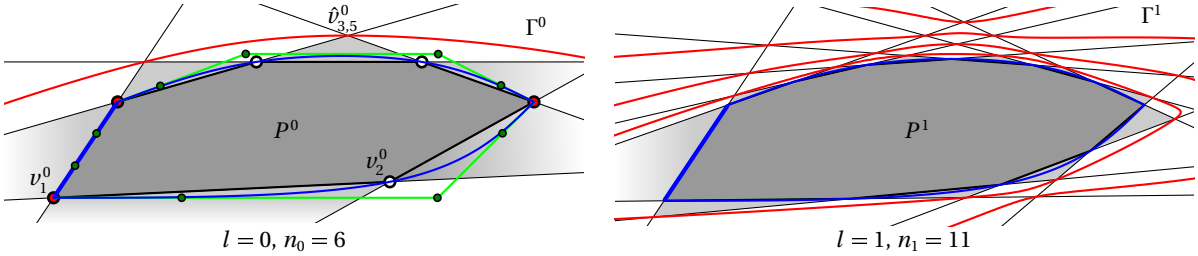

Figure 5: Admissible polygons P^l (dark grey) inscribed in a weakly convex domain Ψ and the associated adjoint curves Γ^l (red) for $l = 0, 1$. The boundary curve of Ψ (blue) is a closed cubic B-spline curve defined by the green control polygon with three corners (red bullets) and a straight segment (thick blue). The adjoint curves touch $\hat{P}^l$ (light grey) at the exterior intersection points $\hat{v}^l_{i-1,i+1}$, but do not intersect $\hat{P}^l$.

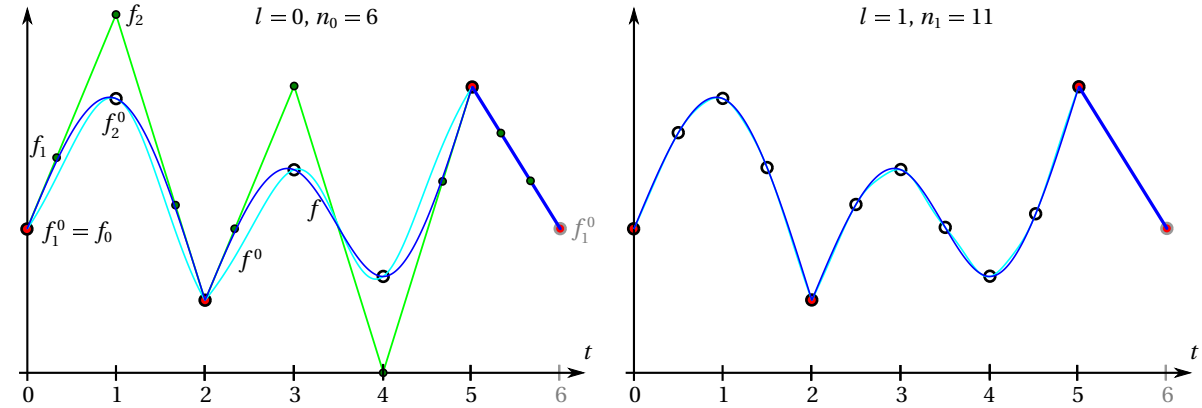

Figure 6: Approximation of the closed B-spline function f (blue) defined by the green control values over the boundary of Ψ (see Figure 5) with three "corners" (red bullets) and a linear segment (thick blue) by the restrictions f^l (cyan) of the discrete Wachspress interpolants to $\partial\Psi$ for $l = 0, 1$.

based on the uniform periodic cubic B-spline function

$$f\colon [0,5] \to \mathbb{R}, \qquad f(t) = \sum_{i=0}^{7} f_i N_i(t),$$

with control values $(f_0, \ldots, f_7) = (1,5,2,0,3,1,5,2)$ and B-spline basis functions as above. We further computed the restrictions $f^l = g^l_{h_l} \circ p$ of the discrete Wachspress interpolants to $\partial\Psi$. Figure 4 shows that f^l is well-defined, smooth, and interpolates f at the vertices of P^l, that is, $f^l(t^l_i) = f^l_i = f(t^l_i)$, $i = 1, \ldots, n_l$.

Figures 5 and 6 show similar examples for a weakly convex domain Ψ, with similar results as expected by Remark 5. More precisely, in both figures the boundary of Ψ is a closed cubic B-spline curve $p\colon [0,6] \to \mathbb{R}^2$, $p(t) = \sum_{i=0}^{12} p_i N_i(t)$ with $p_{12} = p_0$ over the knot vector $(\tau_0, \ldots, \tau_{16}) = (0,0,0,0,1,2,2,2,3,4,5,5,5,6,6,6,6)$. This curve p has three corners p_0, p_4, p_9 at $t = 0$, $t = 2$, $t = 5$, respectively, and it contains the straight segment $[p_9, p_{12}]$ for $t \in [5,6]$. The $n_l = 5 \cdot 2^l + 1$ vertices of the inscribed polygons P^l were generated by uniformly sampling only the interval $[0,5]$ and not $[0,6]$, that is, $v^l_i = p(t^l_i) \in \partial\Psi$ for $t^l_i = (i-1)/2^l$, $i = 1, \ldots, n_l$. Therefore, the straight segment $[p_9, p_{12}]$ appears as the edge $[v_{n_l}, v_1]$ of P^l for any l, and all P^l are admissible. The function f used for the transfinite Wachspress interpolant is a cubic B-spline function $f\colon [0,6] \to \mathbb{R}$, $f(t) = \sum_{i=0}^{12} f_i N_i(t)$ with control values $(f_0, \ldots, f_{12}) = (2,3,5,\frac{7}{3},1,2,4,0,\frac{8}{3},4,\frac{10}{3},\frac{8}{3},2)$ over the same knot vector used for the definition of p.

4 Conclusion and future work

While Kosinka and Bartoň [5] show that discrete Wachspress interpolants converge pointwise to their transfinite counterparts with quadratic rate at any interior point $v \in \Psi$, their approach does not apply to points on the boundary of Ψ. One of the missing ingredients for establishing the convergence on $\partial\Psi$ was that they could only conjecture that Wachspress coordinates and interpolants are well-defined on $\partial\Psi$. Corollary 4

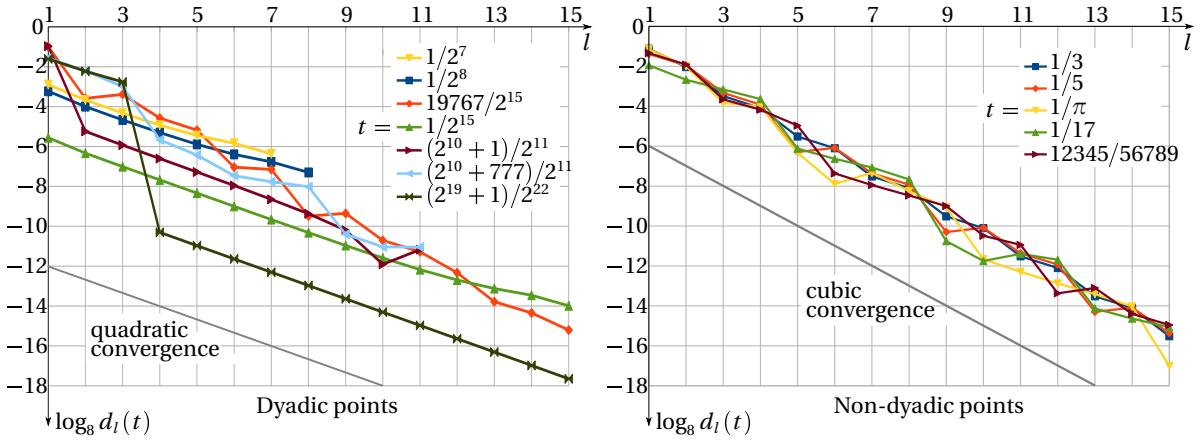

Figure 7: Behaviour of the interpolated values at dyadic (left) and non-dyadic (right) boundary points for the example in Figures 3 and 4. Since $d_l(t) = 0$ for $l > k$ at the dyadic points $t = i/2^k$, some of the sequences in the left plot are truncated accordingly.

now confirms that their conjecture was correct. As mentioned in [5], this is important in applications where the "gap" between $\bar{\Psi}$ and $\bar{P}$ cannot be tolerated.

By Theorem 3 and Proposition 1, Wachspress coordinates and interpolants are actually well-defined over the larger set $\bar{P} \cup \hat{P} \supset \bar{\Psi}$ and even on the boundary of this set, except at the exterior intersection points $\hat{v} \in \hat{V} \subset \Gamma$, which is an important step towards the exact characterization of the connected component of $\mathbb{R}^2$ which contains P and is bounded by Γ. In future work, we plan to attack the same problem of well-definedness in the 3D setting.

Getting back to the convergence issue, we actually studied the approximation rates at the boundary points of Ψ, expecting to see the same pointwise quadratic convergence that occurs at the interior points of Ψ, and made an interesting observation. To be precise, we computed the absolute differences

$$d_l(t) = |f^l(t) - f^{l-1}(t)|, \qquad l \in \mathbb{N}$$

between the values of the discrete Wachspress interpolants at the boundary point $p(t)$ at two consecutive levels for several $t \in [a,b]$. Figure 7 reports the results for the example presented in Figures 3 and 4. The left plot shows the decay of $d_l(t)$ for various *dyadic* boundary points with $t = i/2^k$, which are vertices of P^l for $l \geqslant k$, due to the specific sampling pattern used in this example. Therefore, $f^l(t) = f(t)$ for $l \geqslant k$ and $d_l(t) = 0$ for $l > k$, but for $l \leqslant k$, the decay rate seems to be quadratic. For *non-dyadic* boundary points, however, the right plot suggests that $d_l(t)$ decreases at a cubic rate.

While the distinction between dyadic and non-dyadic points is specific to this particular example, also for more general examples we always observed a quadratic decay rate of $d_l(t)$ for $l \leqslant k$ if there exists some k such that $f_l(t) = f(t)$ for $l \geqslant k$, and a cubic decay rate otherwise. We even considered examples where the inscribed polygons are created by irregular sampling patterns, so that none of the boundary points remains a polygon vertex from some level on, and we still got the cubic rate, this time at *all* boundary points.

Overall, our numerical results, which were all obtained using sequences of admissible inscribed polygons P^l with $O(2^l)$ vertices and maximum parametric distance h_l of order $O(1/2^l)$, suggest that in both cases (non-asymptotic quadratic and asymptotic cubic decay rate), that is, for *any* $t \in [a,b]$, there exists some constant C_t that depends on t, but not on l, such that $d_l(t) \leqslant C_t/8^l$ for $l \in \mathbb{N}$. Noting that

$$|f^l(t) - f(t)| \leqslant \sum_{k=l+1}^{\infty} d_k(t) \leqslant C_t \sum_{k=l+1}^{\infty} \frac{1}{8^k} = \frac{C_t}{7} \cdot \frac{1}{8^l},$$

we therefore conjecture that discrete Wachspress interpolants converge pointwise with cubic rate on the boundary of Ψ, that is,

$$f_h(t) = g_h(p(t)) = f(t) + O(h^3) \qquad \text{as} \qquad h \to 0.$$

But it remains future work to further explore and prove this remarkable behaviour.

Acknowledgements

This work was supported by the SNF under project number 200021_150053. We further thank the anonymous reviewers for their valuable comments and suggestions, which helped to improve this paper.

References

[1] M. S. Floater. Generalized barycentric coordinates and applications. *Acta Numerica*, 24:161–214, 2015.

[2] M. S. Floater and J. Kosinka. Barycentric interpolation and mappings on smooth convex domains. In *Proceedings of the 14th ACM Symposium on Solid and Physical Modeling*, SPM 2010, pages 111–116, 2010.

[3] W. J. Gordon and C. A. Hall. Construction of curvilinear co-ordinate systems and applications to mesh generation. *International Journal for Numerical Methods in Engineering*, 7(4):461–477, 1973.

[4] K. Hormann and M. S. Floater. Mean value coordinates for arbitrary planar polygons. *ACM Transactions on Graphics*, 25(4):1424–1441, Oct. 2006.

[5] J. Kosinka and M. Bartoň. Convergence of Wachspress coordinates: from polygons to curved domains. *Advances in Computational Mathematics*, 41(3):489–505, June 2015.

[6] M. Meyer, H. Lee, A. Barr, and M. Desbrun. Generalized barycentric coordinates on irregular polygons. *Journal of Graphics Tools*, 7(1):13–22, 2002.

[7] T. Sauer. *Numerical Analysis*. Pearson, Boston, second edition, 2012.

[8] E. L. Wachspress. *A Rational Finite Element Basis*, volume 114 of *Mathematics in Science and Engineering*. Academic Press, New York, 1975.

[9] J. Warren. On the uniqueness of barycentric coordinates. In R. Goldman and R. Krasauskas, editors, *Topics in Algebraic Geometry and Geometric Modeling*, volume 334 of *Contemporary Mathematics*, pages 93–100. American Mathematical Society, Providence, 2003.

[10] J. Warren, S. Schaefer, A. N. Hirani, and M. Desbrun. Barycentric coordinates for convex sets. *Advances in Computational Mathematics*, 27(3):319–338, Oct. 2007.